의학석사 학위논문

Dual effects of human adipose tissue-derived mesenchymal stem cells on the NF-κB pathway in tumor growth of A549 lung adenocarcinoma cells and HT-29 colon cancer cells

A549 폐 선암종 세포와 **HT-29** 결장암 세포
성장 기전에서 **NF-κB** 세포신호전달에 대한
인간 지방조직유래 중간엽 줄기세포의
이중효과에 관한 연구

2014년 2월

서울대학교 대학원

의학과 면역학 전공

류 정 주

Dual effects of human adipose tissue-derived mesenchymal stem cells on the NF-κB pathway in tumor growth of A549 lung adenocarcinoma cells and HT-29 colon cancer cells

지도교수 강 병 철

이 논문을 의학석사학위논문으로 제출함

2013년 10월

서울대학교 대학원
의학과 면역학 전공
류 정 주

류정주의 석사학위논문을 인준함

2014년 1월

위 원 장 _____ (인)

부위원장 _____ (인)

위 원 _____ (인)

Dual effects of human adipose tissue-derived mesenchymal stem cells on the NF-κB pathway in tumor growth of A549 lung adenocarcinoma cells and HT-29 colon cancer cells

by

Jung Joo Rhyu

A thesis submitted to the Department of Medicine
in partial fulfillment of the requirements for
the Degree of Master of Science in Medicine (Immunology)
at Seoul National University College of Medicine

January 2014

Approved by Thesis Committee:

Professor _____**Chairman**

Professor _____**Vice Chairman**

Professor _____

학위논문 원문제공 서비스에 대한 동의서

본인의 학위논문에 대하여 서울대학교가 아래와 같이 학위논문 제공하는 것에 동의합니다.

1. 동의사항
① 본인의 논문을 보존이나 인터넷 등을 통한 온라인 서비스 목적으로 복제할 경우 저작물의 내용을 변경하지 않는 범위 내에서의 복제를 허용합니다.

② 본인의 논문을 디지털화하여 인터넷 등 정보통신망을 통한 논문의 일부 또는 전부의 복제.배포 및 전송 시 무료로 제공하는 것에 동의합니다.

2. 개인(저작자)의 의무
본 논문의 저작권을 타인에게 양도하거나 또는 출판을 허락하는 등 동의 내용을 변경하고자 할 때는 소속대학(원)에 공개의 유보 또는 해지를 즉시 통보하겠습니다.

3. 서울대학교의 의무
① 서울대학교는 본 논문을 외부에 제공할 경우 저작권 보호장치(DRM)를 사용하여야 합니다.

② 서울대학교는 본 논문에 대한 공개의 유보나 해지 신청 시 즉시 처리해야 합니다.

논문제목 : A549 폐 선암종 세포와 HT-29 결장암 세포 성장 기전에서 NF-κB 세포신호전달에 대한 인간 지방조직유래 중간엽 줄기세포의 이중효과에 관한 연구

학위구분 : **석사 ■ · 박사 □**
학 과 : 의학과
학 번 :
연 락 처 :
저 작 자 : 류 정 주 (인)

제 출 일 : 2014년 월 일

서울대학교총장 귀하

ABSTRACT

Dual effects of human adipose tissue-derived mesenchymal stem cells on the NF-κB pathway in tumor growth of A549 lung adenocarcinoma cells and HT-29 colon cancer cells

Jung Joo Rhyu, D.V.M.

Department of Medicine

Graduate School of Seoul National University

Human adipose tissue-derived mesenchymal stem cells (hATMSCs) have a great potential as therapy for various diseases and in regenerative medicine. However, emerging evidence suggests that human stem cells have both promoting and inhibitory effects on tumor growth. For the clinical use of hATMSCs as a novel cell therapy, it is important to determine in which tumor environments hATMSCs have tumor supporting effects or suppressing effects and to understand the underlying mechanisms. In this study, hATMSCs affected tumor growth differently depending on the types of tumor cell. Among several types of tumor cell lines, the hATMSCs particularly inhibited the growth of A549 lung adenocarcinoma cells, but promoted the growth of HT-29 colon cancer cells in an *in vivo* xenograft model. Additional results from an *in vitro* study were coincided with the *in vivo* experiment of hATMSCs effects on tumor growth in A549 and HT-29 cell lines. The hATMSCs induced apoptosis and inhibited proliferation of A549 lung cancer cells, but the hATMSCs conversely affected the HT-29 colon cancer cells.

Also, the change in NF-κB expression level after hATMSC treatment was the same in both the *in vivo* and *in vitro* experiments. The expression level of phosphorylated NF-κB p65 was reduced in A549 tumor cells, but the level was increased in HT-29 tumor cells. Altogether, we demonstrated dual effects of hATMSCs, which included an inhibiting effect on A549 and a promoting effect on HT-29. The expression level of NF-κB p65 was correlated with these dual effects in the A549 and HT-29 tumor cell lines.

Keywords: human adipose tissue derived mesenchymal stem cells; tumor; A549 lung cancer cells; HT-29 colon cancer cells; NF-κB; p65

Student number: 2010-23713

CONTENTS

LIST OF FIGURES

LIST OF ABBREVIATIONS

MSCs	mesenchymal stem cells
ATMSCs	adipose tissue derived mesenchymal stem cells
hATMSCs	human adipose tissue derived mesenchymal stem cells
BM-MSCs	bone marrow derived mesenchymal stem cells
SCID	severe combined immunodeficiency
NF-κB	nuclear factor kappa B
IκB	inhibitor of kappa B
IKK	IκB kinase
JAK	janus kinase
STAT	signal transducers and activators of transcription
DKK-1	dickkopf-related protein-1
VEGF	vascular endothelial growth factor
FDGF	fibroblast-derived growth factor
SDF-1	stromal derived factor-1
Ang1	angiopoietin-1
IL-6	interleukin 6
TNF-α	tumor necrosis factor alpha
CCL5	chemokine ligand 5

INTRODUCTION

Mesenchymal stem cells (MSCs) can be found in various tissues, including bone marrow, umbilical cord blood, placenta, and fat (1). MSCs are defined as cells possessing abilities for self-renewal, proliferation, and differentiation into multiple lineages, including chondrocytes, osteoblasts, and adipocytes (2). Among diverse tissue sources of MSCs, adipose tissue is accessible and abundant for the isolation of adult stem cells. Therefore, human adipose tissue derived MSCs are an very attractive source for cell therapy. They can expand multiply and be obtained by relatively less invasive procedures.

MSCs are also known to have homing properties and repair injured tissues, thus MSCs have appeal as a potential therapy for regenerative medicine, organ defects, or certain other conditions. Many studies have shown that MSCs are potential treatment for various conditions such bone defects (3, 4), hair loss (5), liver fibrosis (6), pancreatic islet transplantation (7), immunomodulation (7), and neuronal regeneration (8).

Meanwhile, recent evidence suggests that MSCs could also play a role in carcinogenesis progression and the modulation of tumor growth and metastasis, although these potential effects remain controversial and not fully understood. Many opposing results have been reported from separate studies and some results indicate inhibitory effects on tumor growth and development. Maestroni *et al.* reported that the coinjection of mouse BM-MSCs inhibited the proliferation and growth of tumor cells in Lewis lung carcinoma and B16 melanoma (9). Khakoo *et al.* injected human BM-MSCs systematically and

found a tumor-suppressive effect in an experimental model of Kaposi Sarcoma (10). It was also reported by Cousin *et al.* that the growth of Capan-1 pancreatic cancer cells was inhibited by the injection of hATMSCs. In contrast, a promotion effect of MSCs on tumor growth was observed in other studies. Zhu *et al.* subcutaneously injected human BM-MSCs together with colon cancer cells (SW480 and F6), which promoted angiogenesis and tumor growth (11). It was also reported by Djouad *et al.* that the interaction of mouse BM-MSCs and the melanoma cell line B16 enhanced the incidence of tumor formation (12). Xu *et al.* reported that human BM-MSCs promoted growth and metastasis of osteosarcoma (Saos-2) (13). In another case reported by Tian *et al.* there were opposite effects of MSCs *in vivo* and *in vitro,* in which human BM-MSCs exerted a tumor inhibitory effect *in vitro,* but surprisingly had a promoting effect on tumor growth *in vivo* in A549 and Eca-109 tumor cells (1).

Some mechanisms of these MSC-related tumor supporting effects have been reported, which include vascular support, tumor stromal support, immunosuppressive effects, and metastatic support. First, MSCs have been reported to differentiate into endothelial cells (14) and secrete vasculogenic growth factors (15). In some cases MSCs support tumor growth by differentiating into tumor stromal fibroblasts (16). MSCs are also known to have an immunosuppressive effect (17), which eventually helps tumor formation and growth. And finally, MSCs are known to secret factors such as CCL-5 which induces metastasis (18). On the other hand, the tumor inhibition mechanisms of MSCs were may be due to cell cycle arrest, angiogenesis

inhibition, and certain soluble factors that may block tumor related cell signaling pathways. Tumor cell cycle arrest was reported as a mechanism of MSC-related tumor cell inhibition (19). In addition, the anti-angiogenesis effect of MSCs in cancer was referred to as another mechanism (20). Finally, MSCs are known to secrete soluble factors, such as the Wnt inhibitor, DKK-1, which can inhibited tumor cell growth and reduced survival factors of cancer, such as β-catenin, c-Myc, and survivin (21, 22).

Despite these explanations regarding the action of MSCs, the tumor modulation mechanism of MSCs is very complicated and difficult to demonstrate. Still, MSCs are showing different effects on tumor progression in research. Thus, in order for clinical use of MSCs as a novel cell therapy for various conditions, it is critical to understand the interactions between tumor cells and MSCs.

In this study, we investigated the supporting and suppressing effects of hATMSCs using several types of human cancer xenograft mouse models to clarify the effects of hATMSCs on human cancers and determine the underlying mechanism.

MATERIALS AND METHODS

Tumor cell lines

Six kinds of tumor cell lines were used. The A-375, A549, and HT-29 cell lines were purchased from ATCC (Manassas, VA, USA) and the A-431, NCI-N87, and Capan-1 cell lines were purchased from the Korean Cell Line Bank (Seoul, Korea). A-375 is derived from human malignant melanoma, A-431 is derived from human epidermoid carcinoma, A549 is derived from lung carcinoma, HT-29 is derived from colorectal adenocarcinoma, NCI-N87 is derived from gastric carcinoma, and Capan-1 is derived from pancreatic adenocarcinoma, which were cultured in RPMI1640 (GIBCO, Grand Island, NY, USA) supplemented with 10% FBS (GIBCO, Grand Island, NY, USA) and 0.03% antibiotic-antimycotic (GIBCO, Grand Island, NY, USA). The cells were subcultured at 70~80% confluency and were maintained and grown at 37°C in a 5% CO_2 humidified chamber.

Isolation and characterization of hATMSCs

The test material in this study, human adipose tissue derived mesenchymal stem cells (hATMSCs),was provided by K-STEMCELL (Seoul, Korea). The hATMSCs were acquired by following a previously reported process (23). The adipose tissue was obtained by liposuction of abdominal subcutaneous fat from human donors. The subcutaneous adipose tissues were digested with collagenase I (1 mg/mL) under gentle agitation at 37°C for 1 hr. The digested

tissues were filtered through a 100 μm nylon sieve to remove cellular debris and centrifuged at 470 g for 5 min. The pellet was resuspended in DMEM (Invitrogen, Carlsbad, CA, USA)-based media containing 0.2 mM ascorbic acid and 10% FBS. The cell suspension was re-centrifuged at 470 g for 5 min. The supernatant was discarded and the cell pellet was collected. The cell fraction was cultured overnight at 37°C and 5% CO_2 in DMEM-based media containing 0.2 mM ascorbic acid and 10% FBS. Cell adhesion was checked under an inverted microscope the next day. After 24 hr, non-adherent cells were removed and washed with PBS. The cell medium was changed to Keratinocyte-SFM (Invitrogen)-based media containing 0.2 mM ascorbic acid, 0.09 mM calcium, 5 ng/mL recombinant epidermal growth factor (rEGF), and 5% FBS. The cells were maintained for four or five days until they became confluent, and were considered at this point to represent passage 0. At the confluency of 90%, the cells were subculture-expanded in Keratinocyte-SFM-based media containing 0.2 mM ascorbic acid, 0.09 mM calcium, 5 ng/mL rEGF, and 5% FBS until passage 3. The immunophenotypes of the hATMSCs were analyzed. Trypsinized hATMSCs were suspended (1×10^6 hATMSCs/25 μl of PBS). The cells were stained with 2 μl of fluorescence conjugated antibodies, FITC-conjugated CD31, CD34, CD45 (BD Pharmingen, San Diego, CA, USA) antibodies, and PE-conjugated CD73, CD90 (BD Pharmingen, San Diego, CA, USA) antibodies. After staining, the cells were suspended in 200 μl of PBS. The immunophenotype was analyzed using a FACS Calibur flow cytometer (Becton Dickinson, San Jose, CA, USA) using Cell Quest software. Viability was assessed by the trypan blue exclusion assay.

Before shipping, cell viability was over 95% and there was no evidence of bacterial, fungal, or mycoplasmal contamination. The procedures for MSC were performed by K-STEMCELL (Seoul, Korea) under good manufacturing practice (GMP) conditions.

In vivo tumor xenograft model

Six-week old female balb/c-nude mice were purchased from Orient Bio (Seong-nam, Gyeonggi, Korea). All animals were housed in an air-conditioned room under a proper temperature (22±2°C), adequate humidity (40-60%), and a 12-hour light cycle. All animal experiments were approved by the Institutional Animal Care and Use Committee (IACUC) of the Biomedical Research Institute at Seoul National University Hospital (approval No. : 11-0148, 12-0170).

The mice were transplanted with 6 types of tumor cell lines, A375, A431, A549, NCI-N87, HT-29, and Capan-1. The tumor cells were suspended in PBS and 5×10^6 tumor cells in 100μl of PBS were inoculated subcutaneously into the backs of nude mice. When tumor volume reached close to 100 mm^3 after tumor inoculation, the mice in each tumor group were divided into 2 groups: a control group and a treatment group.

Every experimental group of mice was treated with an intratumoral injection of hATMSCs (1×10^5 hATMSCs/10μl PBS) once a week for 8 weeks and each control group was given a PBS (10μl) injection. The intratumoral injections were performed with a sterile, 31G insulin syringe. Tumor size was measured twice a week using a caliper (Mitutoyo, Japan) and tumor volumes were

calculated as π/6(length x width x height). After 8 weeks of injection and observation, the animals were sacrificed and the tumor masses were removed. Tumor weights were measured and each tumor mass was sampled and fixed in 10% neutral buffered formaldehyde solution for histological analysis or preserved in -70°C for western blot analysis.

In vitro coculture and trypan blue exclusion assay

Cell viability was detected by a trypan blue exclusion assay. A549 and HT-29 tumor cells were cocultured with hATMSCs directly or indirectly for 72 hr and cell growth was assessed by the total number of live cells.

Direct coculture

The A549 and HT-29 tumor cells (1×10^5 cells) were cocultured with hATMSCs in RPMI1640 media with 10% FBS. Each set of tumor cells was plated in 6-well plates in the presence of hATMSCs at different ratios, 10:0.5, 10:1, and 10:2, or not in the presence of hATMSCs. All experiments were conducted in triplicate and the cultures were kept at 37℃ and 5% CO_2 for 72 hr. After incubation, the cocultured cells were harvested by Trypsin EDTA treatment and centrifugation and the cell pellets were suspended in 1 mL of PBS. Total cell number was assessed by a trypan blue exclusion assay using a haemocytometer under a microscope.

Indirect coculture

Indirect coculture was conducted using transwell membranes to prevent cell-

to-cell contact. Transwell inserts (0.4 μm pore, polycarbonate membrane; SPL, Korea) in 6-well plates were used. The indirect coculture of tumor cells was performed in the presence of hATMSCs at different ratios, 10:0.5, 10:1, and 10:2, or not in the presence of hATMSCs. Each A549 and HT-29 cell suspension (1×10^5 cells/2 ml media) was put into the lower compartment of the culture well, and the hATMSC suspensions or just media alone were loaded into the upper inserts. After 72 hr of incubation, the cocultured tumor cells in the lower compartment were harvested and the number of tumor cells was assessed by trypan blue staining and counted with a haemocytometer.

Western blot analysis

Western blot analysis was performed for assessing the expression level of tumor-related cell signaling pathway proteins such as phosphorylated NF-κB p65, phosphorylated JAK3, phosphorylated STAT3, and β-Catenin. The proteins were extracted from *in vivo* tumor specimens of A549 and HT-29 using RIPA lysis buffer (Millipore, Bedford, MA, USA) containing 0.1% phosphatase inhibitor cocktails (Sigma-Aldrich, St. Louis, MO, USA) and one tablet of protease inhibitor (protease inhibitor Roche, Indianapolis, IN, USA). The protein concentrations were determined using a BCA protein assay kit (Pierce Biotechnology, N. Meridian Road, Rockford, USA). Each protein lysate sample was run on a 10% SDS-polyacrylamide gel at 110V for 1 hr 40 min and electrophoretically transferred to a polyvinylidene fluoride membrane (Immun-Blot, Bio-Rad, Richmond, CA, USA) at 100V for 1 hr at 4°C. The membranes were blocked with 5% skim milk (BD, Franklin Lakes, NJ, USA)

in TBST buffer for 1 hr. Each membrane was incubated overnight at 4°C with different antibodies, phosphorylated NF-κB p65 antibody (1:1,000, Cell signaling Technology), p-JAK3 antibody (1:500, Santa Cruz Biotechnology, CA, USA), p-STAT3 antibody (1:500, Santa Cruz Biotechnology, CA, USA), β-Catenin(1:1,000, Santa Cruz Biotechnology, CA, USA), and β-actin antibody (1:1,000, Cell signaling Technology). The membranes were washed with TBST buffer and incubated with secondary antibody, a goat anti-rabbit IgG conjugated with horseradish peroxidase (1:5,000, Santa Cruz Biotechnology, CA, USA). Then, the membranes were again washed with TBST buffer and protein bands were visualized by a enhanced chemiluminescence kit. The relative band intensity was quantified using the free Image J program from the National Institutes of Health (Bethesda, MD, USA).

Histopathological analysis

Immunohistochemistry

For immunohistochemistry, 5-μm sections of tumor tissue were deparaffinized and processed by an indirect immunoperoxidase method using monoclonal antibodies specific for NF-κB p65 (1:500, Cell Signaling Technology). Microwave antigen retrieval was performed in pH 6.0 citrate buffer (Target Retrieval Solution, Dako, Denmark) for 20 min. The sections were sequentially treated with 3% H_2O_2 in PBS for 10 min. For the primary antibody reaction, slides were incubated for 1 hr at 37°C in a wet chamber in

a 1:500 dilution of NF-κB p65 (Cell Signaling Technology) antibody. Then the sections were treated with peroxidase labeled polymer conjugated to goat anti-rabbit immunoglobulins in Tris-HCl buffer, and were visualized by staining with 3,3'-diaminobenzidine (DAB) chromogen solution in the substrate buffer solution (EnVision Dual Link System-HRP, Dako, USA). Finally, the sections were counterstained with hematoxylin.

TUNEL staining

In situ detection of DNA fragmentation was performed using a TUNEL staining kit, the ApopTag® Peroxidase *In Situ* Apoptosis Detection Kit (Millipore, Bedford, MA, USA) according to the manufacturer's instructions. After being washed 3 times in Tris-HCl (pH 7.7), sections were treated with 2 % H_2O_2 for 10 min at room temperature to block endogenous peroxidase activity. The sections were then incubated with terminal deoxynucleotidyl transferase enzyme solution at 37℃ for 1 hr. The sections were dipped in 10 mM sodium citrate buffer (pH 6.0) for 15 min at room temperature to terminate the reaction. The sections were washed 3 times in Tris-HCl (pH 7.7) and subsequently blocked with PBS (pH 7.4) containing 10% normal goat serum and 0.3% Triton X-100. Biotinylated-16-dUTP was visualized by the ABC (avidin-biotin complex) method with 0.05% 3,3'-diaminobenzidine (DAB) and 0.005% H_2O_2. Methyl green was used for counterstaining.

Flow cytometry analysis

Analysis of NF-κB expression level

After indirect coculture for 72 hr with hATMSCs, tumor cells were harvested and analyzed by a flow cytometer (FACS Calibur, Becton Dickinson, San Jose, CA, USA) to assess levels of proliferation, apoptosis, necrosis, and NF-κB expression level. All experiments were conducted in triplicate.

Harvested tumor cells were centrifuged and resuspended in PBS and fixed in 2~4% formaldehyde. After fixation, the tubes were chilled on ice and then permeabilized in 90% methanol for 30 min on ice. At least 0.5×10^6 cells per sample were aliquoted into each assay tube and washed twice with incubation buffer. Each sample was resuspended in 100 ul of incubation buffer and blocked for 10 min at room temperature. Phospho-NF-κB p65-Alexa Fluor 647 Conjugate (1:50, Cell Signaling Technology) antibody was added to each assay tube and incubated for 1 hr at room temperature. The cells were rinsed and resuspended in 0.5 mL of PBS and analyzed using a FACS Calibur (Becton Dickinson, San Jose, CA, USA) with BD Cell Quest Pro 3.3.0.software.

Analysis of apoptosis and proliferation

After indirect coculture of the tumor cells and hATMSCs, annexin V/propidium iodide double staining was conducted for assessment of apoptosis and necrosis, and BrdU labeling was performed for evaluation of proliferation. An Annnexin V-FITC Early Apoptosis Detection Kit (Cell

Signaling Technology) and BrdU Flow Kit (FITC BrdU Flow Kit , BD Pharmingen) were used by following the manufacturer's instructions. Flow cytometric analysis was performed on a FACS Calibur (Becton Dickinson, San Jose, CA, USA) using the BD Cell Quest Pro 3.3.0.software program.

Statistical analysis

The data were expressed as means±SD values. The statistical analysis on results was performed using a one-way ANOVA (SPSS software for window version 21.0; SPSS) or Student's *t*-test was used for single statistical comparisons. *P* values ≤ 0.05 were considered statistically significant.

RESULTS

Immunophenotype of hATMSCs

For the immunophenotypic characterization of hATMSCs, the surface markers expression was examined by flow cytometry. The hATMSCs expressed high level of CD73 and CD90, whereas hATMSCs were negative for CD31, CD34, and CD45 (Fig. 1).

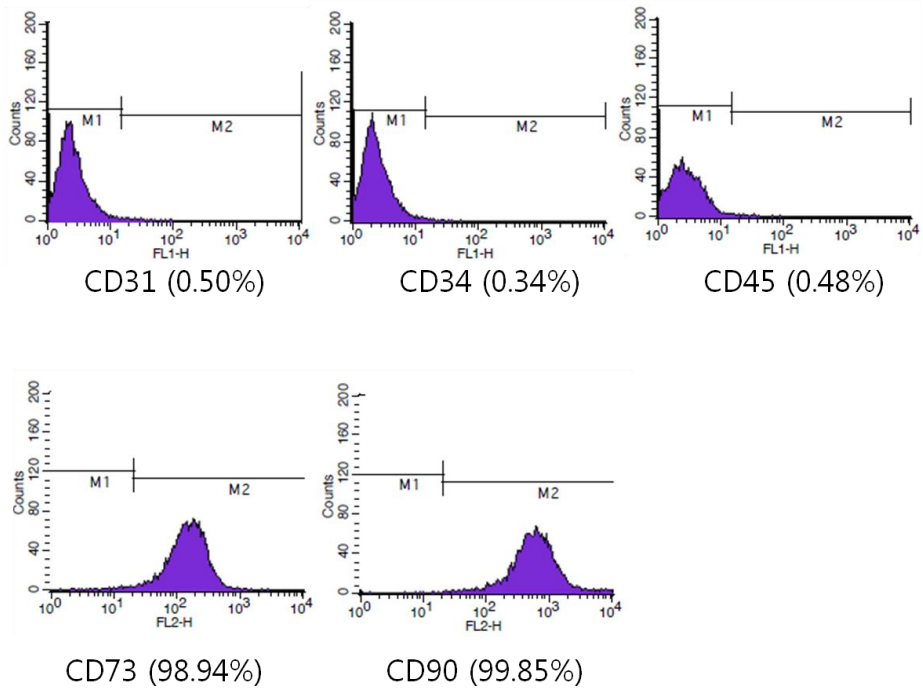

Figure 1. Flow cytometric characterization of hATMSCs. The hATMSCs were harvested at passage 3 and labeled with the antibodies specific for the indicated hATMSCs surface antigens. The number in parenthesis indicates percentage of surface marker positive cells.

The effect of hATMSCs on the growth of various types of tumors in an in vivo xenograft model

Tumor size and weights were measured to investigate the effect of hATMSCs on the growth of various tumor cell lines, including A375, A431, A549, NCI-N87, HT-29, and Capan-1 (Fig. 2). Each treatment group was administered with 1×10^5 of hATMSCs. The injection of hATMSCs helped to decrease the mean volumes and weights of the tumor cell lines A431, Capan-1, and A549 (Fig. 2A, 2B, 2C, and 2G). Particularly, in the A549 tumor models, the hATMSCs-treated tumors were smaller than the control group tumors in size and weight following 8 weeks of treatment (Fig. 2C). On the other hand hATMSCs treatment increased the mean volume and weight in the tumor cell lines NCI-N87, A375, and HT-29 (Fig. 2D, 2E, 2F, and 2G). Especially in the HT-29 tumor xenograft model, the tumor weight in the hATMSCs-treated group was dramatically increased compare to that in the control group with statistical significance (Fig. 2F). We focused on 2 types of tumors, A549 and HT-29, and conducted an additional *in vivo* experiment using Hairless SCID mice and confirmed similar dual effects with statistical significance for both tumors. The volumes and weights of the A549 tumors were smaller compared to those of the control group following hATMSCs treatment, whereas the volumes and weights of the hATMSCs-treated HT-29 tumors were greater than those of the control group tumors (Fig. 3).

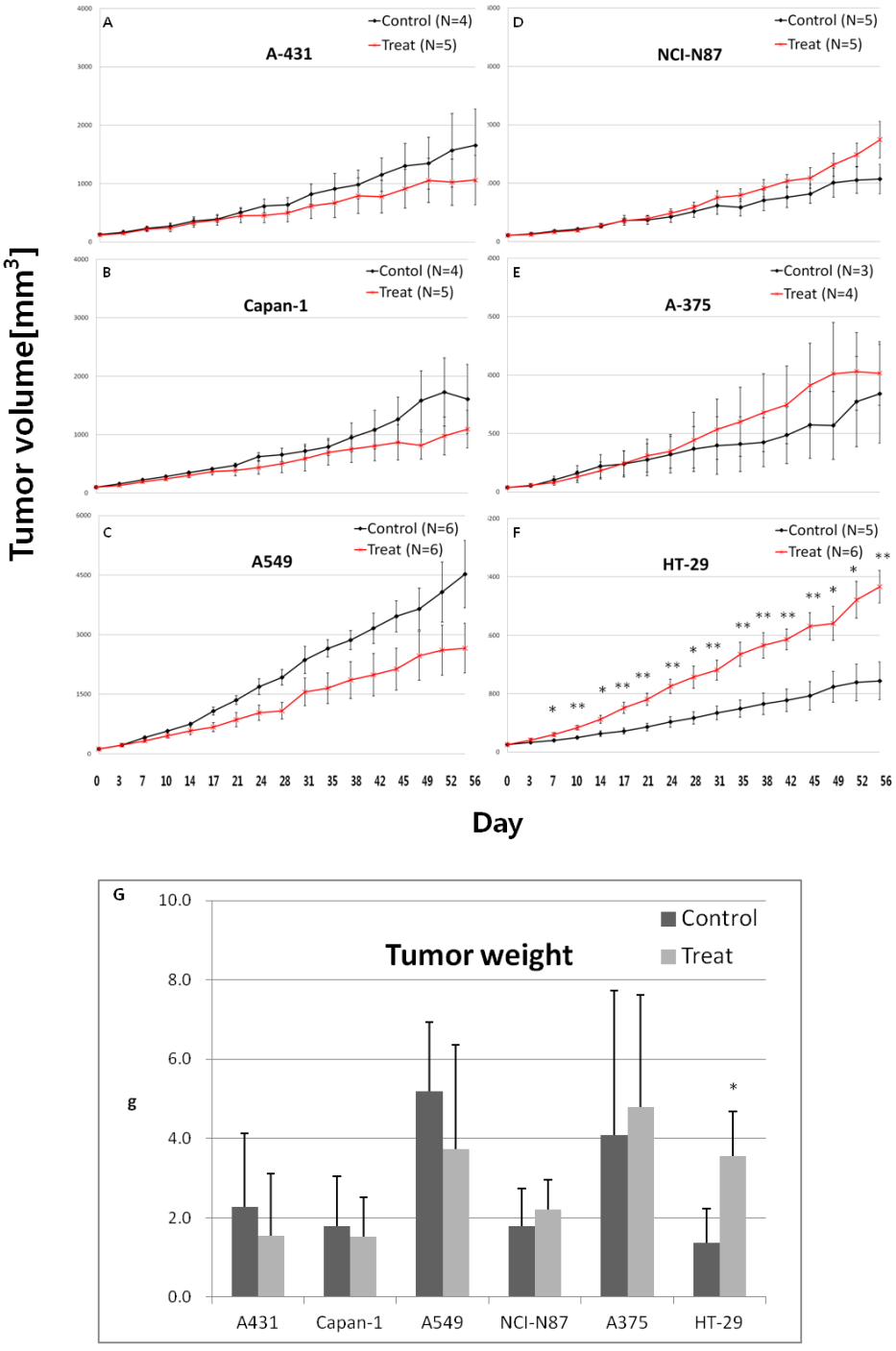

Figure 2. Tumor growth affected by treatment of hATMSCs in various tumor models using nude mice. A. A-431, derived from human epidermoid

carcinoma B. Capan-1, derived from pancreatic adenocarcinoma C. A549, derived from lung carcinoma D. NCI-N87, derived from gastric carcinoma E. A-375, derived from human malignant melanoma F. HT-29, derived from colorectal adenocarcinoma G. The change in tumor weights following hATMSCs injection in a nude mice xenograft model. The results are presented as the mean ± SD for tumor weight and mean ± SE (standard error) for tumor volume. Asterisks indicate a statistically significant difference from the control group (*$P < 0.05$, **$P < 0.01$).

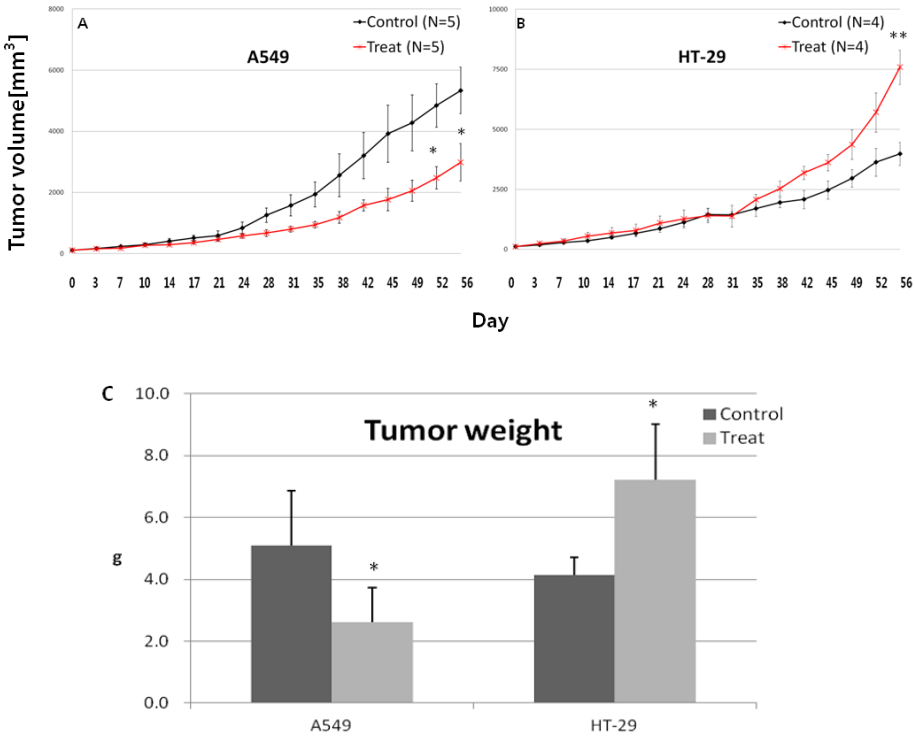

Figure 3. Tumor growth affected by treatment of hATMSCs in A549 and HT-29 tumor xenograft models using hairless SCID mice model. A. A549, derived from lung carcinoma B. HT-29, derived from colorectal adenocarcinoma C. The change in tumor weights following hATMSCs injection in the hairless SCID mice model. Results are presented as the mean ± SD for tumor weight and mean ± SE (standard error) for tumor volume growth. Asterisks indicate a statistically significant difference from the control group (*P < 0.05, **P < 0.01).

Molecular changes of phosphorylated NF-κB p65 in A549 and HT-29 tumors induced by the hATMSCs treatment

The proteins extracted from the xenograft tumor mass were analyzed by western blot analysis to investigate if there is a correlation between certain cell signaling pathways and hATMSC affected tumor growth. Among several proteins related to cell signaling pathways, the activation level of NF-κB was affected by hATMSCs. The treatment of hATMSCs reduced the expression level of phosphorylated p65 approximately 31% in A549, whereas expression was promoted approximately 77% in HT-29 tumors (Fig. 4A, 4B). Other cell signaling related proteins, such as p-JAK3 and p-STAT3 were not affected significantly and the β-Catenin expression level was elevated in HT-29 tumor by hATMSCs treatment, but not affected in A549 tumor (Fig. 4A). The changes in NF-κB p65 expression level in the treatment group coincided with tumor growth, which was reduced in A549, but at the same time increased in HT-29.

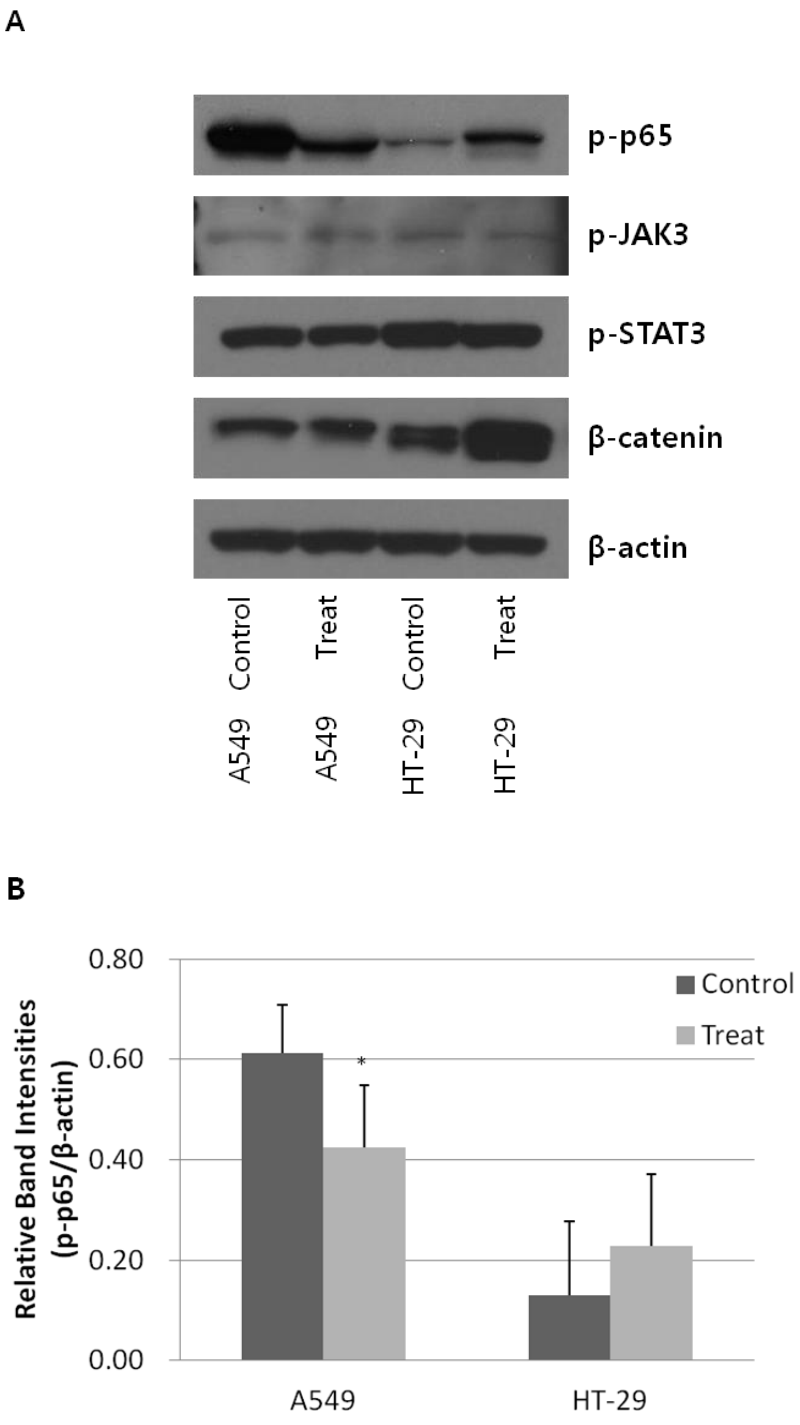

Figure 4. Molecular changes by hATMSCs in A549 and HT-29 tumor masses. A. The expression levels of phosphorylated NF-κB p65, p-JAK3, p-STAT3, β-Catenin and β-actin were detected by western blotting. B. The mean of

relative band intensities of phosphorylated NF-κB p65 expression. Results are presented as the mean ± SD and asterisks indicate a statistically significant difference from the control group (*$P < 0.05$).

Histopathological changes in A549 and HT-29 tumors following hATMSC treatment

After the *in vivo* xenograft study, each tumor was sampled and apoptosis changes affected by hATMSCs were detected by TUNEL staining. In the hATMSC-treatment groups, apoptosis was increased in A549 (Fig. 5A, 5B) but decreased in HT-29 (Fig. 5C, 5D) compared to the control groups. In addition, the change in expression level of NF-κB p65 by hATMSCs was detected using immunohistochemistry. The immunopositive area of p65 was reduced in the A549 tumors (Fig. 5E, 5F), wheareas it was increased in HT-29 by hATMSCs treatment (Fig. 5G, 5H).

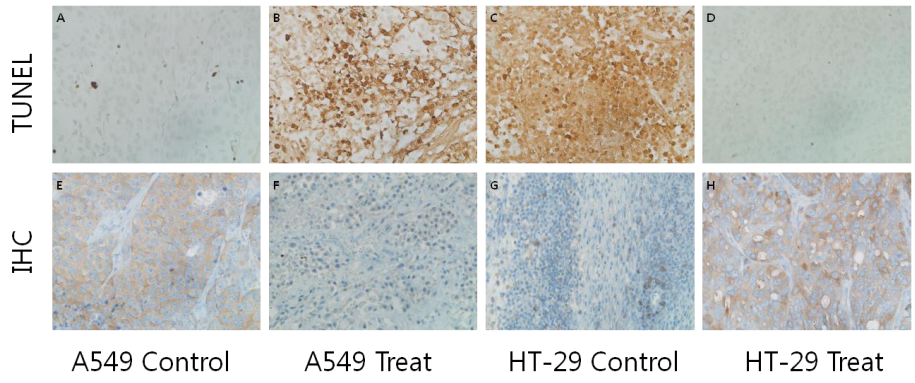

Figure 5. Histopathological analysis of *in vivo* xenograft tumor masses of A549 and HT-29 using TUNEL staining and immunohistochemistry. A~D. Apoptosis detection in both control and treatment groups of A549 and HT-29(x 400). E~H. Detection for immunopositive areas of NF-κB p65 in both control and treatment groups of A549 and HT-29(x 400).

The effect of hATMSCs on the cell viability of tumor cell lines, A549 and HT-29 in vitro

In vitro coculture of tumor cells and hATMSCs confirmed similar effects as the *in vivo* xenograft studies of tumor growth using A549 and HT-29 tumors. Each tumor cell line, A549 and HT-29, was cocultured with hATMSCs at different ratios of 10:0.5, 10:1, and 10:2, respectively.

In direct coculture, the hATMSCs exerted an inhibitory effect on A549 tumor growth and a promoting effect on HT-29 tumor growth. At the ratios of 10:1 and 10:2, the proliferation rates of A549 cells were reduced 9.78 % and 19.82 %, respectively, compared to the control, and proliferation rates of HT-29 increased 17.22% and 29.78%, respectively (Fig. 6A, 6B).

The same impact was also observed in indirect coculture using cell inserts. The hATMSCs had similar dose dependent dual effects on A549 and HT-29. At the ratios of 10:1 and 10:2 of indirect coculture, the proliferation rates of A549 were reduced 9.72% and 18.57%, respectively compared to the control, and those of HT-29 increased 19.90% and 25.79 %, respectively (Fig. 6C, 6D). There was a statistical significance at the ratio of 10:2 in the A549 coculture system and at the ratios of 10:1 and 10:2 in the HT-29 coculture system, but there was no drastic effect at the ratio of 10:0.5.

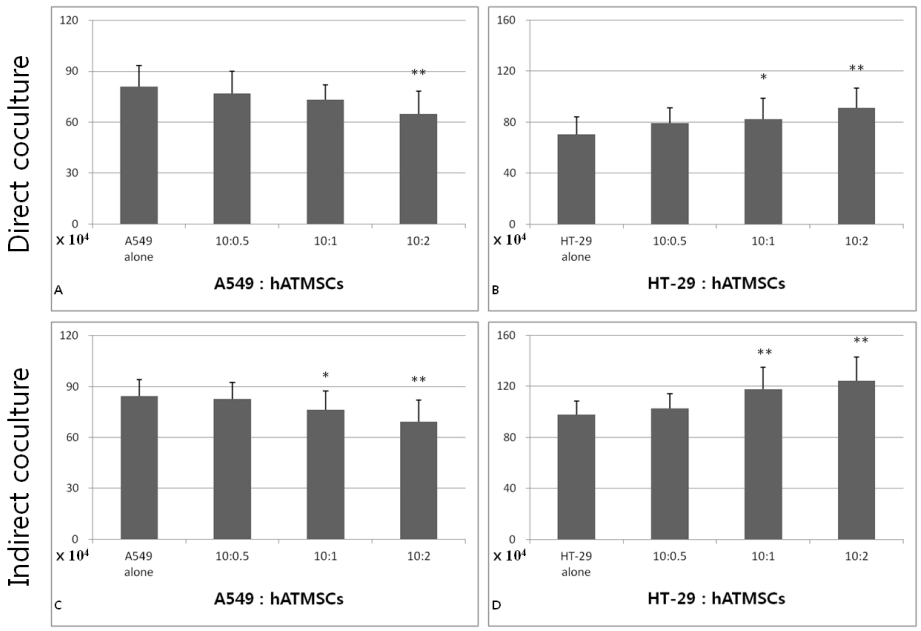

Figure 6. The number of live cells in direct or indirect coculture of tumor cells and hATMSCs. The coculture with hATMSCs significantly reduce the number of live cells of A549 and increased that of HT-29 cells at the ratios of 10:0.5, 10:1, and 10:2 (Tumor cells : hATMSCs). A. The number of viable cells in the direct coculture system of A549 and hATMSCs, B. The number of viable cells in the direct coculture system of HT-29 and hATMSCs, C. The number of viable cells in the indirect coculture system of A549 and hATMSCs, D. The number of viable cells in the indirect coculture system of HT-29 and hATMSCs. All data represent means±SD and asterisks indicate a statistically significant difference from the control group (*$P < 0.05$, **$P < 0.01$).

The coculture effect of hATMSCs on the tumor cell apoptosis and proliferation

The proliferation levels of hATMSC-cocultured tumor cells were measured by BrdU staining and flow cytometry analysis. The BrdU-positive cells in A549 were reduced by hATMSCs-coculture by approximately 34% and 23% at the ratios of 10:1 and 10:2, respectively (Fig. 7A). On the other hand, there was s a slight increase in cocultured HT-29 cells (Fig. 7B). The rates of apoptotic and live cells of hATMSC-cocultured tumor cells were analyzed by annexin V/PI double staining and flow cytometry analysis. The rate of live cells was decreased significantly in A549 by hATMSCs-coculture (Fig. 8D), but rates of apoptotic cells were elevated 40%, 85%, and 95% at the ratios of 10:0.5, 10:1, and 10:2, respectively (Fig. 8B). However, hATMSCs had opposite effects with the HT-29 cells, where there was an increase in live cells (Fig. 8E) and decreases in apoptotic cells of 23% and 26% at the ratios of 10:1 and 10:2, respectively (Fig. 8C).

Taken together, hATMSCs assumably have two opposite effects on A549 and HT-29 tumor cells. The treatment of hATMSCs may inhibit proliferation but elevate apoptosis in A549, but on the other hand promote the proliferation and reduce apoptosis in HT-29.

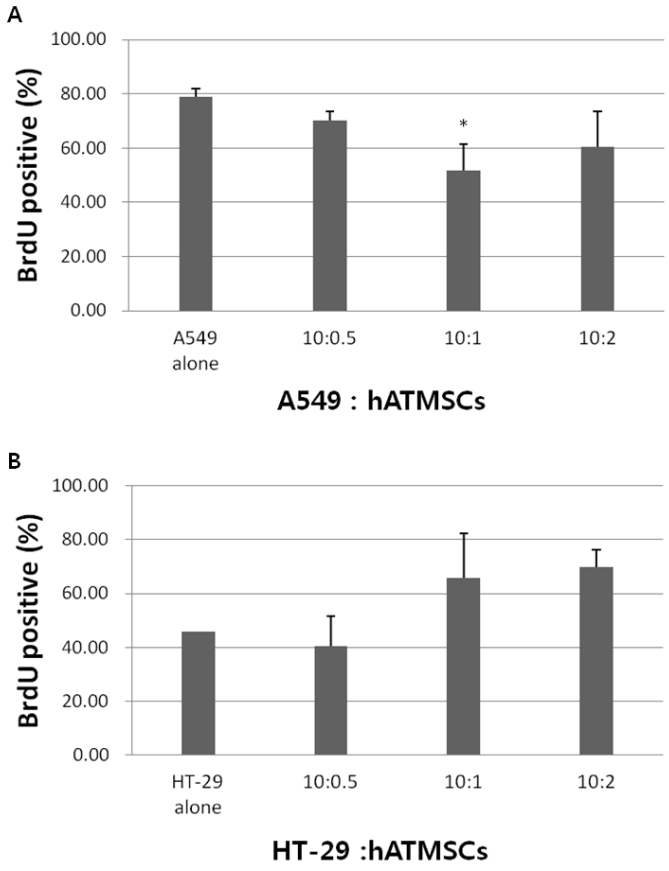

Figure 7. The proliferation rates of A549 and HT-29 tumor cells cocultured with hATMSCs. The coculture with hATMSCs significantly attenuated the growth of A549 cells and increased the growth of HT-29 cells A. BrdU positive cells in A549 B. BrdU positive cells in HT-29. All experiments were conducted in triplicate. Results represent means±SD and asterisks indicate a statistically significant difference from the control group (*$P < 0.05$).

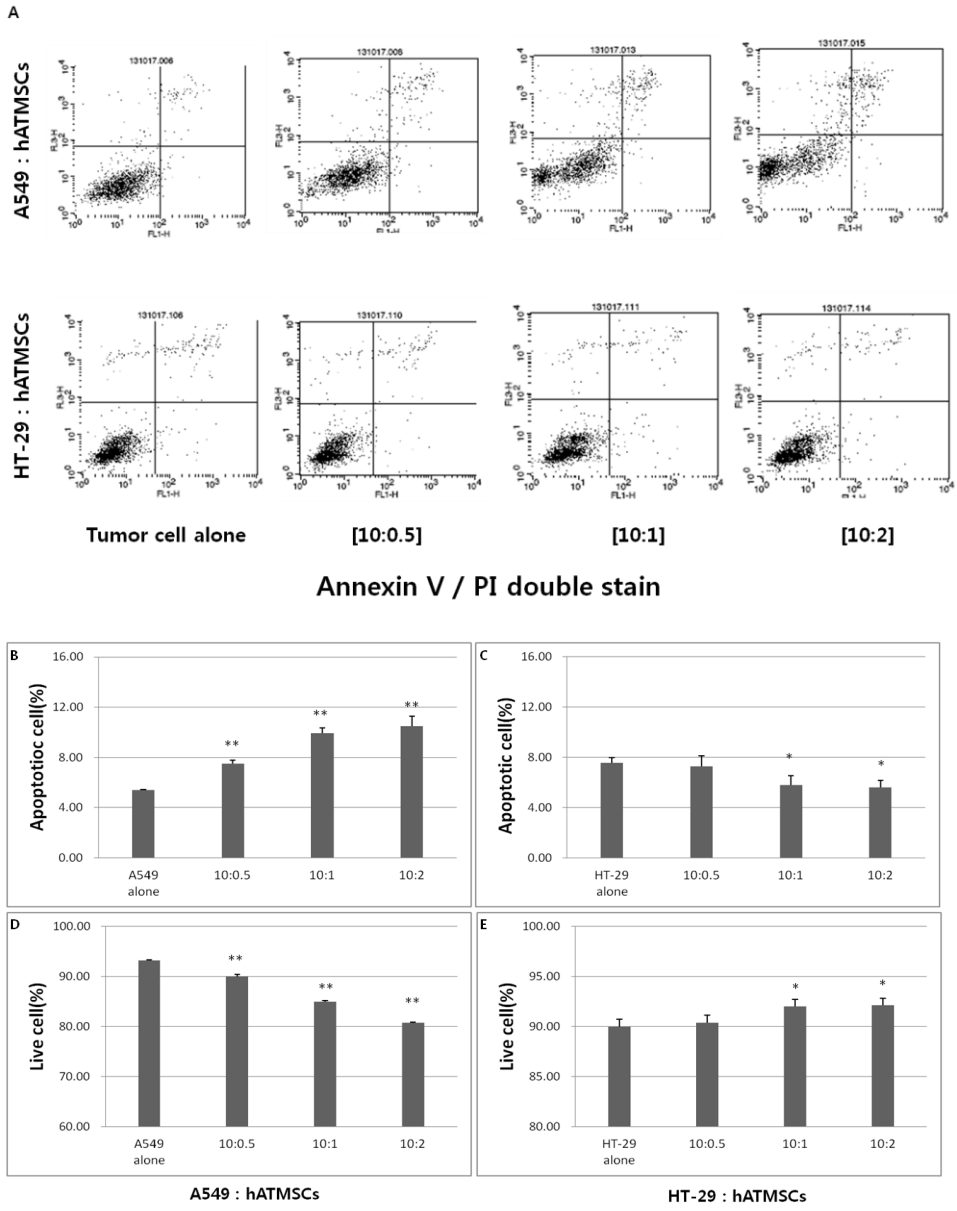

Figure 8. Annexin V/PI double staining and detection of apoptosis. A. Annexin V/PI double staining and flow cytometric analysis for the detection of apoptosis in tumor cells of A549 and HT-29 following coculture with hATMSCs. B. The rate of apoptotic cells in A549 after coculture with hATMSCs, C. The rate of apoptotic cells in HT-29 after coculture with

hATMSCs, D. The rate of live cells in A549 after coculture with hATMSCs, E. The rate of live cells in HT-29 after coculture with hATMSCs. Apoptotic cells include annexin V(+)PI(+) cells and annexin V(+)PI(-) cells. All experiments were conducted in triplicate. Results represent means±SD and asterisks indicate a statistically significant difference from the control group (*$P < 0.05$, **$P < 0.01$).

The coculture effect of hATMSCs on the phosphorylated NF-κB p65 expression in A549 and HT-29 tumor cell lines

The expression level of phosphorylated NF-κB p65 was quantified in A549 and HT-29 tumor cells after coculture with hATMSCs. The flow cytometric analysis for phosphorylated NF-κB p65 (Alexa Fluor 647 Conjugate) revealed a significant reductions in A549, approximately 12%, 25%, and 32% at the ratios of 10:0.5, 10:1, and 10:2, respectively (Fig. 9A). However, there was a reverse effect in the HT-29 cells, with a profound elevation in phosphorylated NF-κB p65 expression of about 15% at the ratio of 10:2 (Fig. 9B).

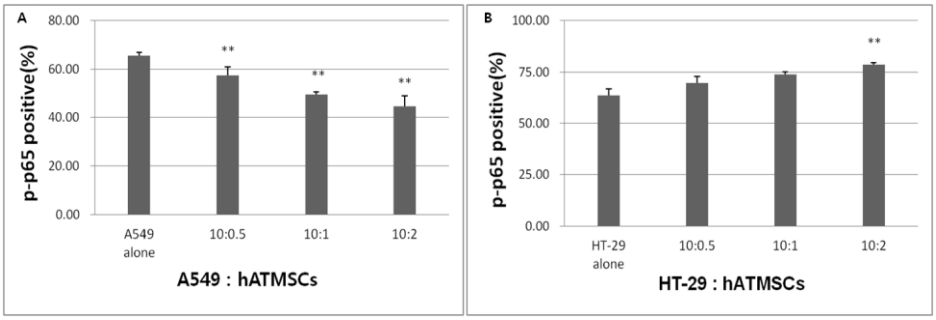

Figure 9. Flow cytometry analysis for phosphorylated NF-κB p65. A. p-p65 expression level in A549 was decreased by coculture of hATMSCs dose dependently. B. p-p65 expression level in HT-29 was increased. The experiment was performed twice with triplicate determinations. Results are presented as the mean ± SD and asterisks indicate a statistically significant difference from the control group (n=6 per group, $*P < 0.05$, $**P < 0.01$).

DISCUSSION

Mesenchymal stem cells have great potential as a novel therapy for regenerating tissues and organs or injured areas. Moreover, human MSCs have recently been reported to have modulation properties in tumor progression. Interestingly, many studies have reported contradicting results, with some investigators finding that MSCs promote tumor growth and others reporting that MSCs inhibit tumor growth (24).

In this study, we tried to investigate the tumor-modulation effects of hATMSCs, which have been studied relatively less in cancer research compared to BM-MSCs. To determine the effects of hATMSCs on human cancer, we applied hATMSCs to 6 different types of tumor xenograft models. Even though MSCs express tumor tropism, Seo *et al.* reported in 2011 that intratumoral injection of MSCs was most effective, in which tumor growth was smaller in an intratumoral injection group compared to subcutaneous and intravenous injection groups (25). Therefore, we chose the intratumoral injection route for hATMSC application *in vivo*. Additional *in vitro* studies were conducted that specifically focused on A549 and HT-29 tumor cells using coculture systems. Altogether, the hATMSCs showed dual effects such as a strong inhibition effect on A549 and a dramatic promotion effect on HT-29 tumor growth both *in vivo* and *in vitro*.

There have been reports on the effects of BM-MSCs, particularly on A549 and HT-29 tumor cells. Li *et al.* reported that BM-MSCs have an inhibitory effect on A549 lung cancer cells, both in *in vivo* and *in vitro* experiments (26).

Reversely, the tumor-promotion effect of BM-MSCs was demonstrated by Tsai *et al.* In their study BM-MSCs promoted tumor formation of HT-29 colorectal cancer cells (27).

Moreover, cell signaling pathways have been referenced in order to explain the mechanisms of the effects of MSCs on tumors. The PI3K/AKT(28) pathway was referred to by Ma *et al.* as a possible means of cell signaling related to tumor-inhibition effects of umbilical cord MSCs. The WNT pathway (21) and the JAK/STAT pathway (27) were also suggested as being related to the effects of MSCs. We investigated certain protein expressions to determine which cell signaling pathway may be related to MSC effects on tumor growth. After detection of protein expressions by western blot analysis, we found that the expression level of NF-κB p65 was related to tumor growth or inhibition. The expression level of NF-κB p65 level was inhibited in A549 tumor cells, but at the same time promoted in HT-29 tumor cells.

The nuclear factor kappa B (NF-κB) family is known to control the inflammatory response and apoptosis. Generally, NF-κB pathway activation is triggered in response to microbial and viral infections or exposure to pro-inflammatory cytokines that activate the IKK complex, leading to IκB degradation and finally translocation of p50/p65 heterodimers into the nucleus. When activated, the NF-κB signaling pathway regulates a variety of downstream genes that govern immunity, inflammation, cell growth, and apoptosis (29).

In the tumor environment, the NF-κB cell signaling pathway is widely known to regulate the growth and metastasis of various tumors. Even with A549 and

HT-29 tumor cells a correlation was reported in which cell proliferation was promoted by activation of the NF-κB pathway and suppressed by blocking the NF-κB cell signaling pathway (30, 31). NF-kB acts through the transcription of anti-apoptotic proteins, leading to increased proliferation of cells and tumor growth (32). Aberrant sustained activation of NF-κB has been implicated in various stages of cancer (33, 34). As a potent safeguard of tumors, NF-κB induces anti-apoptotic activity in tumor cells. Therefore, blocking the NF-κB pathway is regarded as a necessary addition to the future of cancer therapy (35).

Some researchers have tried to explain the interaction of tumors and MSCs and tumors involving the NF-κB signaling pathway. Uchibori *et al.* claimed that the activation of the NF-κB signaling pathway induces the accumulation of MSCs at tumor sites by inducing VCAM-1 in MSCs and thereby their interaction with tumor vessel endothelial cells (36). Their study indicates that direct cell-to-cell interaction between tumor cells and MSCs is responsible for the effects of MSCs on tumors. Meanwhile, others claim that tumors are regulated by secreted soluble factors from MSCs. Fierro *et al.* reported that both direct and indirect interactions between MSCs and breast cancer cells enhanced tumor cell proliferation (37). Similarly, in our experiments using *in vitro* coculture systems, the same effects of hATMSCs were confirmed both in direct and indirect coculture systems. This indicates that even without direct cell-to-cell contact, MSCs can affect tumor cell growth and hATMSCs might influence cancer cell growth by their soluble factors in conditioned medium.

Many MSC-releasing soluble factors have been revealed. For example, MSCs are known to secrete various tumor regulating factors. Among these factors, proangiogenic factors are released by MSCs, such as VEGF (37), FDGF (38, 39), SDF-1 (38, 39), and Ang1 (40). These cytokines promote endothelial and smooth muscle migration and proliferation at the tumor site, facilitating angiogenesis. Also, there are factors such as IL-6 and TNF-α (41) that are produced by MSCs and have immunosuppressive effects and eventually tumor supporting effects. Karnoub *et al.* reported that MSC-secreted CCL5 induced a transient prometastatic effect on breast cancer cells (18). CCL5 secreted by MSCs and chemokine receptor 5 expression in breast cancer cells were found to be critical for the prometastatic effect of MSCs (18, 24). On the other hand, the tumor inhibitory effects of MSCs are known to be mediated by DKK-1, which is secreted by MSCs and exhibits an inhibiting effect on β-catenin signaling (21). Adipose tissue derived MSCs were also found to inhibit proliferation in primary leukemia cells by secreting DKK-1 (22, 24).

Despite previous reports on tumor modulation mechanisms and regulating factors of MSCs, the exact mechanism remains unclear. Further studies are necessary to analyze the factors released from hATMSCs in conditioned medium and investigate which factors contribute to the function of hATMSCs, in order to understand the interaction between MSCs and cancer cells and the involvement of the NF-κB signaling pathway.

Altogether, our work represents the first study showing that hATMSCs have two different effects depending on the type of tumor. Given the possibility of MSCs as a novel therapeutic tool for various diseases, it is critical to explain

for the conflicting findings in tumor-MSC studies. Our results suggest a dual modulation effect of hATMSCs and their possible role in the NF-κB pathway. Based on the current results, investigations of the involvement of the tumor-microenvironment and hATMSC-releasing factors may lead to a novel application strategy of stem cell based therapy.

Acknowledgments

The adipose tissue derived mesenchymal stem cells (hATMSCs) used in this study were produced and kindly provided by K-STEMCELL Co., Ltd, Korea.

REFERENCES

1. L.L. Tian, W. Yue, F. Zhu, S. Li, and W. Li. Human mesenchymal stem cells play a dual role on tumor cell growth *in vitro* and *in vivo*. J Cell Physiol. 226:1860-1867 (2011).
2. M. Dominici, K. Le Blanc, I. Mueller, I. Slaper-Cortenbach, F. Marini, D. Krause, R. Deans, A. Keating, D. Prockop, and E. Horwitz. Minimal criteria for defining multipotent mesenchymal stromal cells. The International Society for Cellular Therapy position statement. Cytotherapy. 8:315-317 (2006).
3. J. Dong, T. Uemura, Y. Shirasaki, and T. Tateishi. Promotion of bone formation using highly pure porous beta-TCP combined with bone marrow-derived osteoprogenitor cells. Biomaterials. 23:4493-4502 (2002).
4. H.J. Choi, J.M. Kim, E. Kwon, J.H. Che, J.I. Lee, S.R. Cho, S.K. Kang, J.C. Ra, and B.C. Kang. Establishment of efficacy and safety assessment of human adipose tissue-derived mesenchymal stem cells (hATMSCs) in a nude rat femoral segmental defect model. Journal of Korean medical science. 26:482-491 (2011).
5. K.E. Toyoshima, K. Asakawa, N. Ishibashi, H. Toki, M. Ogawa, T. Hasegawa, T. Irie, T. Tachikawa, A. Sato, A. Takeda, and T. Tsuji. Fully functional hair follicle regeneration through the rearrangement of stem cells and their niches. Nature communications. 3:784 (2012).
6. K.W. Seo, S.Y. Sohn, D.H. Bhang, M.J. Nam, H.W. Lee, and H.Y.

Youn. Therapeutic effects of hepatocyte growth factor-overexpressing human umbilical cord blood-derived mesenchymal stem cells on liver fibrosis in rats. Cell Biol Int (2013).

7. M. Perez-Basterrechea, A.J. Obaya, A. Meana, J. Otero, and M.M. Esteban. Cooperation by fibroblasts and bone marrow-mesenchymal stem cells to improve pancreatic rat-to-mouse islet xenotransplantation. PLoS One. 8:e73526 (2013).

8. E. Bas, T.R. Van De Water, V. Lumbreras Cruz, S. Rajguru, G. Goss, J.M. Hare, and B. Goldstein. Adult human nasal mesenchymal-like stem cells restore cochlear spiral ganglion neurons after experimental lesion. Stem Cells Dev (2013).

9. G.J. Maestroni, E. Hertens, and P. Galli. Factor(s) from nonmacrophage bone marrow stromal cells inhibit Lewis lung carcinoma and B16 melanoma growth in mice. Cellular and molecular life sciences : CMLS. 55:663-667 (1999).

10. A.Y. Khakoo, S. Pati, S.A. Anderson, W. Reid, M.F. Elshal, Rovira, II, A.T. Nguyen, D. Malide, C.A. Combs, G. Hall, J. Zhang, M. Raffeld, T.B. Rogers, W. Stetler-Stevenson, J.A. Frank, M. Reitz, and T. Finkel. Human mesenchymal stem cells exert potent antitumorigenic effects in a model of Kaposi's sarcoma. J Exp Med. 203:1235-1247 (2006).

11. W. Zhu, W. Xu, R. Jiang, H. Qian, M. Chen, J. Hu, W. Cao, C. Han, and Y. Chen. Mesenchymal stem cells derived from bone marrow favor tumor cell growth *in vivo*. Experimental and molecular pathology. 80:267-274 (2006).

12. F. Djouad, P. Plence, C. Bony, P. Tropel, F. Apparailly, J. Sany, D. Noel, and C. Jorgensen. Immunosuppressive effect of mesenchymal stem cells favors tumor growth in allogeneic animals. Blood. 102:3837-3844 (2003).

13. W.T. Xu, Z.Y. Bian, Q.M. Fan, G. Li, and T.T. Tang. Human mesenchymal stem cells (hMSCs) target osteosarcoma and promote its growth and pulmonary metastasis. Cancer Lett. 281:32-41 (2009).

14. A. Al-Khaldi, N. Eliopoulos, D. Martineau, L. Lejeune, K. Lachapelle, and J. Galipeau. Postnatal bone marrow stromal cells elicit a potent VEGF-dependent neoangiogenic response *in vivo*. Gene therapy. 10:621-629 (2003).

15. B.D. Roorda, A. ter Elst, W.A. Kamps, and E.S. de Bont. Bone marrow-derived cells and tumor growth: contribution of bone marrow-derived cells to tumor micro-environments with special focus on mesenchymal stem cells. Critical reviews in oncology/hematology. 69:187-198 (2009).

16. P.J. Mishra, R. Humeniuk, D.J. Medina, G. Alexe, J.P. Mesirov, S. Ganesan, J.W. Glod, and D. Banerjee. Carcinoma-associated fibroblast-like differentiation of human mesenchymal stem cells. Cancer Res. 68:4331-4339 (2008).

17. J. Plumas, L. Chaperot, M.J. Richard, J.P. Molens, J.C. Bensa, and M.C. Favrot. Mesenchymal stem cells induce apoptosis of activated T cells. Leukemia. 19:1597-1604 (2005).

18. A.E. Karnoub, A.B. Dash, A.P. Vo, A. Sullivan, M.W. Brooks, G.W.

Bell, A.L. Richardson, K. Polyak, R. Tubo, and R.A. Weinberg. Mesenchymal stem cells within tumour stroma promote breast cancer metastasis. Nature. 449:557-563 (2007).

19. Y.R. Lu, Y. Yuan, X.J. Wang, L.L. Wei, Y.N. Chen, C. Cong, S.F. Li, D. Long, W.D. Tan, Y.Q. Mao, J. Zhang, Y.P. Li, and J.Q. Cheng. The growth inhibitory effect of mesenchymal stem cells on tumor cells in vitro and in vivo. Cancer Biol Ther. 7:245-251 (2008).

20. K. Otsu, S. Das, S.D. Houser, S.K. Quadri, S. Bhattacharya, and J. Bhattacharya. Concentration-dependent inhibition of angiogenesis by mesenchymal stem cells. Blood. 113:4197-4205 (2009).

21. L. Qiao, Z.L. Xu, T.J. Zhao, L.H. Ye, and X.D. Zhang. Dkk-1 secreted by mesenchymal stem cells inhibits growth of breast cancer cells via depression of Wnt signalling. Cancer Lett. 269:67-77 (2008).

22. Y. Zhu, Z. Sun, Q. Han, L. Liao, J. Wang, C. Bian, J. Li, X. Yan, Y. Liu, C. Shao, and R.C. Zhao. Human mesenchymal stem cells inhibit cancer cell proliferation by secreting DKK-1. Leukemia. 23:925-933 (2009).

23. J.C. Ra, I.S. Shin, S.H. Kim, S.K. Kang, B.C. Kang, H.Y. Lee, Y.J. Kim, J.Y. Jo, E.J. Yoon, H.J. Choi, and E. Kwon. Safety of intravenous infusion of human adipose tissue-derived mesenchymal stem cells in animals and humans. Stem Cells Dev. 20:1297-1308 (2011).

24. A.H. Klopp, A. Gupta, E. Spaeth, M. Andreeff, and F. Marini, 3rd. Concise review: Dissecting a discrepancy in the literature: do

mesenchymal stem cells support or suppress tumor growth? Stem Cells. 29:11-19 (2011).

25. S.H. Seo, K.S. Kim, S.H. Park, Y.S. Suh, S.J. Kim, S.S. Jeun, and Y.C. Sung. The effects of mesenchymal stem cells injected via different routes on modified IL-12-mediated antitumor activity. Gene therapy. 18:488-495 (2011).

26. L. Li, H. Tian, Z. Chen, W. Yue, S. Li, and W. Li. Inhibition of lung cancer cell proliferation mediated by human mesenchymal stem cells. Acta biochimica et biophysica Sinica. 43:143-148 (2011).

27. K.S. Tsai, S.H. Yang, Y.P. Lei, C.C. Tsai, H.W. Chen, C.Y. Hsu, L.L. Chen, H.W. Wang, S.A. Miller, S.H. Chiou, M.C. Hung, and S.C. Hung. Mesenchymal stem cells promote formation of colorectal tumors in mice. Gastroenterology. 141:1046-1056 (2011).

28. Y. Ma, X. Hao, S. Zhang, and J. Zhang. The in vitro and in vivo effects of human umbilical cord mesenchymal stem cells on the growth of breast cancer cells. Breast Cancer Res Treat. 133:473-485 (2012).

29. R.O. Escarcega, S. Fuentes-Alexandro, M. Garcia-Carrasco, A. Gatica, and A. Zamora. The transcription factor nuclear factor-kappa B and cancer. Clin Oncol (R Coll Radiol). 19:154-161 (2007).

30. J. Zhang, Y.J. Xu, W.N. Xiong, Z.X. Zhang, C.L. Du, L.F. Qiao, W. Ni, and S.X. Chen. Inhibition of NF-kappaB through IkappaBalpha transfection affects invasion of human lung cancer cell line A549. Chinese journal of cancer. 27:710-715 (2008).

31. L. Kulikova, J. Mikes, M. Hyzdalova, G. Palumbo, and P. Fedorocko. NF-kappaB is not directly responsible for photoresistance induced by fractionated light delivery in HT-29 colon adenocarcinoma cells. Photochemistry and photobiology. 86:1285-1293 (2010).

32. E. Pikarskyand Y. Ben-Neriah. NF-kappaB inhibition: a double-edged sword in cancer? Eur J Cancer. 42:779-784 (2006).

33. A.S. Baldwin. Control of oncogenesis and cancer therapy resistance by the transcription factor NF-kappaB. J Clin Invest. 107:241-246 (2001).

34. B. Rayetand C. Gelinas. Aberrant rel/nfkb genes and activity in human cancer. Oncogene. 18:6938-6947 (1999).

35. M.W. Mayoand A.S. Baldwin. The transcription factor NF-kappaB: control of oncogenesis and cancer therapy resistance. Biochim Biophys Acta. 1470:M55-62 (2000).

36. R. Uchibori, T. Tsukahara, H. Mizuguchi, Y. Saga, M. Urabe, H. Mizukami, A. Kume, and K. Ozawa. NF-kappaB activity regulates mesenchymal stem cell accumulation at tumor sites. Cancer Res. 73:364-372 (2013).

37. F.A. Fierro, W.D. Sierralta, M.J. Epunan, and J.J. Minguell. Marrow-derived mesenchymal stem cells: role in epithelial tumor cell determination. Clinical & experimental metastasis. 21:313-319 (2004).

38. I.A. Potapova, G.R. Gaudette, P.R. Brink, R.B. Robinson, M.R. Rosen, I.S. Cohen, and S.V. Doronin. Mesenchymal stem cells support migration, extracellular matrix invasion, proliferation, and survival of

endothelial cells in vitro. Stem Cells. 25:1761-1768 (2007).

39. T. Kinnaird, E. Stabile, M.S. Burnett, C.W. Lee, S. Barr, S. Fuchs, and S.E. Epstein. Marrow-derived stromal cells express genes encoding a broad spectrum of arteriogenic cytokines and promote in vitro and in vivo arteriogenesis through paracrine mechanisms. Circ Res. 94:678-685 (2004).

40. L. Qiao, Z. Xu, T. Zhao, Z. Zhao, M. Shi, R.C. Zhao, L. Ye, and X. Zhang. Suppression of tumorigenesis by human mesenchymal stem cells in a hepatoma model. Cell research. 18:500-507 (2008).

41. M.T. Abdel aziz, M.F. El Asmar, H.M. Atta, S. Mahfouz, H.H. Fouad, N.K. Roshdy, L.A. Rashed, D. Sabry, A.A. Hassouna, and F.M. Taha. Efficacy of mesenchymal stem cells in suppression of hepatocarcinorigenesis in rats: possible role of Wnt signaling. J Exp Clin Cancer Res. 30:49 (2011).

국 문 초 록

A549 폐 선암종 세포와 HT-29 결장암 세포 성장 기전에서 NF-κB 세포신호전달에 대한 인간 지방조직유래 중간엽 줄기세포의 이중효과에 관한 연구

서울대학교 대학원 의학과 면역학 전공

류 정 주

인간 지방조직유래 중간엽 줄기세포는 재생의학 및 다양한 질병의 새로운 치료제로서 다양한 가능성을 가지고 있다. 한편, 최근에 발표되는 논문들은 인간 지방조직유래 중간엽 줄기세포가 종양성장에 있어 억제작용 또는 촉진작용을 두 가지 작용을 할 수 있음을 근거하고 있다. 인간 지방조직유래 중간엽 줄기세포를 새로운 치료법으로서 임상적용을 하기 위해서는 그 전에 어떠한 종양환경에서 억제작용 또는 촉진작용을 하는지 알고 그에 대한 메커니즘을 이해하는 것이 필수적이다. 본 연구에서는 6 가지 종양세포주, A-375, A-431, A549, NCI-N87, HT-29, Capan-1 에서 인간 지방유래 중간엽 줄기세포가 종양 성장에 미치는 영향을 *in vivo* xenograft 모델을 이용하여 측정하였다. 인간 지방조직유래 중간엽

줄기세포는 A549 종양은 성장을 억제시켰지만 HT-29 종양은 성장을 촉진시켰다. *In vivo* 연구를 바탕으로 A549 폐 선암종 세포주와 HT-29 결장암 세포주를 *in vitro* 에서 인간 지방유래 중간엽 줄기세포와 함께 direct 또는 indirect coculture 를 시행하였다. 인간 지방유래 중간엽 줄기세포는 A549 의 증식 억제, 세포자멸사 증가 효과가 있었고 HT-29 에서는 증식 촉진 및 세포자멸사 감소 효과가 있었다. 이러한 현상과 관련된 세포신호전달 기전을 알기 위해 웨스턴블롯을 통하여 종양 관련 세포신호전달 단백질의 변화를 분석하였다. 인산화 NF-κB p65, 인산화 JAK3, 인산화 STAT3, β-Catenin 등의 변화를 분석하였고 그 중 NF-κB 관련 단백질이 종양의 성장에 연관성이 있다는 것을 알 수 있었다. 인간 지방유래 중간엽 줄기세포가 A549 종양에서는 NF-κB 세포신호의 subunit 인 인산화 p65 의 발현을 억제시켰고, HT-29 종양에서는 증진시켰다. 위 결과는 인간 지방유래 중간엽 줄기세포의 작용이 두 가지 종양세포주, A549 및 HT-29 종양에 대하여 각기 다르며 인간 지방조직유래 중간엽 줄기세포가 종양에 미치는 영향이 NF-κB 세포신호전달과 연관성이 있음을 보여준다.

주요어: 인간 지방조직유래 중간엽 줄기세포, 종양, A549, HT-29, NF-κB, p65

학 번: 2010-23713